A Study on the Performance of Carbon Sleeve in Continuous Annealing Furnace

JEN-YUNG HSU*, CHIA-HSIANG PENG and YU-SHENG LIN****

**New Materials Research and Development Department*
***Rolling Mill Department III*
China Steel Corporation

A hearth roller in a continuous annealing furnace consists of a carbon sleeve and a metal core cylinder. The carbon sleeve is made of graphite materials and undergoes proper antioxidation treatments to improve its resistance to oxidation at elevated temperatures. In the present study, a variety of carbon sleeves were fabricated to investigate the crucial properties that affect the performance of the rollers. The graphite materials impregnated with phosphate compounds were found to be an effective method for enhancing their antioxidation ability. However, during field tests, the phosphate compounds deposited in the carbon sleeves were prone to hydrolysis, and phosphoric acids leached out. The metal cores of the rollers were thus corroded. The corrosion mechanism was deduced based on the morphology and chemical compositions of the collected rust. The graphite materials with silicon as an antioxidant were also examined. The introduced silicon was rarely able to fill the voids within the graphite, and its antioxidation ability was not as good as that of phosphate compounds as an antioxidant. Even so, the carbon sleeves with silicon antioxidants exhibited sufficient oxidation resistance during field tests. Moreover, no hydrolysis of the antioxidants occurred, which could otherwise have deteriorated the antioxidation resistance of the rollers. Therefore, the graphite materials with silicon deposition were considered a promising candidate for the carbon sleeves.

Keywords: Carbon sleeve, Antioxidation treatment, Continuous annealing furnace

1. INTRODUCTION

A hearth roller is a crucial part of a continuous annealing furnace for silicon steel production[1]. The roller typically consists of a cylindrical metal core and a carbon sleeve. The carbon sleeve is usually made of graphite materials, which have low hardness, good self-lubricity, and adequate mechanical strength at elevated temperatures. These properties make it well-suited for conveying steel strip in the furnace. However, graphite materials are prone to oxidation above 600°C, and the oxidation reaction accelerates significantly when the temperature exceeds 750°C in ambient conditions. In addition, graphite can react with water above 800°C, which is detrimental to the durability of the carbon sleeves.

In most cases, the continuous annealing furnace for silicon steel is operated at elevated temperatures higher than 800°C, but common graphite materials struggle to resist oxidation at such high temperatures. The carbon sleeves are usually subjected to antioxidant treatments before application on the production line. The widely used methods for antioxidant treatments include the introduction of silicon carbide into the carbon sleeve by chemical vapor infiltration[2], and impregnation with phosphate compounds[3] or boric acids[4].

In the present work, several antioxidative carbon sleeves were supplied by renowned bulk graphite suppliers. The physical properties, microstructures, and performance as hearth rollers in the continuous annealing furnace were evaluated, and the efficacy of the corresponding antioxidation treatments was also discussed.

2. EXPERIMENTAL METHODS

2.1 Sample Description and Characterization

H company in Taiwan has provided three types of carbon sleeves, which are denoted as A-H, B-H, and C-H. The other samples were acquired from D company (denoted as D-D), W company (denoted as E-W), and T company (denoted as F-T), respectively. All the samples had already undergone antioxidation treatments. The samples obtained were then cut into suitable dimensions for measuring physical properties. In addition, their microstructures were examined using scanning electron microscopy (SEM; JSM-IT100, JEOL) to

investigate the antioxidation treatments. The introduced antioxidant for each carbon sleeve has been summarized in Table 1, and the detailed analysis is elaborated in the following sections.

Fourier transform infrared (FT-IR) spectroscopy was also applied to investigate the chemical compositions of the sleeves. The spectra were recorded using FT-IR absorption spectrometry (VARIAN 3600, Varian Inc.) in the frequency range of 4000-600 cm^{-1}. The samples to be examined were milled, mixed with KBr powder, pressed into pellets, and then subjected to FT-IR scans.

2.2 Oxidation Kinetics and Field Test

To discern the samples' oxidation resistance ability, the oxidation rate of each sample was examined using a thermal-gravimetric analyzer (TGA; STA7200, Hitachi). The samples were cut into small pieces with the dimensions of 2 × 2 × 2 mm^3. The specimens were rapidly heated at a rate of 20°C/min up to 800°C in N_2 atmosphere, followed by isothermal for 1 h in air to conduct oxidation reaction. The samples' weight loss as a function of time was recorded, and the oxidation rate was thus calculated. Some carbon sleeves with superior oxidation resistance ability could therefore be identified and were deployed in No. 3 Annealing & Coating Line (3ACL) for field testing.

3. RESULTS AND DISCUSSION

3.1 Sample Characterization

Some physical properties of the sleeves obtained were measured and listed in Table 1. All the sleeves in the present study have a density higher than 1.70 g cm^{-3}, indicating that those carbon sleeves are likely made of specialty graphite. The microstructures of those samples were also probed with SEM to assess the antioxidation treatment technologies, and Figure 1 shows the micrographs obtained. The yellow arrows indicate the possible antioxidants deposited. All the samples' micrographs show obvious infiltrated materials except for E-W. This suggests that E-W has not been properly treated, such that no antioxidants remained in the bulk graphite.

Figure 1 also shows that the primary particle size of the deposit materials in A-H, B-H, and C-H is small, and the antioxidants tend to entirely seal the voids of the bulk graphite. By contrast, the particle size of the deposit materials in D-D is larger, and they only loosely fill the voids. For the F-T sample, even though the particle size of the deposit materials is small, the antioxidants just randomly precipitate within the voids rather than seal them. Obviously, the morphologies of the antioxidation-treated carbon sleeves are quite different, suggesting that the suppliers might use different antioxidant chemicals for treatments.

To further explore the antioxidation technologies applied to these samples, SEM equipped with energy dispersive X-ray spectroscopy (SEM-EDX) was used to analyze the chemical elements of the deposit materials. The resultant micrographs and EDX maps are shown in Figure 2. The EDX maps show that A-H, B-H, C-H, and D-D have been impregnated with phosphorus compounds, while F-T was treated with silicon compounds.

The FT-IR spectra of B-H and D-D samples were acquired and depicted in Figure 3. The B-H and D-D samples exhibit vibration bands between 1100 and 850 cm^{-1}, attributed to P-O or P-O-H groups of phosphate compounds of HPO_4^{3-}, PO_4^{3-}, or $H_2PO_4^-$ [5]. Their FT-IR profiles also have two prominent peaks featuring the existence of the phosphate compounds, namely the vibration band at 1105 cm^{-1} from the P-O-P group and the other band at 1285 cm^{-1} from the P=O group[6]. Although the antioxidants within B-H and D-D were both phosphate compounds, their chemical compositions were slightly different. The phosphate compound deposited in B-H was composed mainly of phosphorus (P) and aluminum (Al), while that in D-D was composed of phosphorus (P), oxygen (O), and calcium (Ca) as revealed in Figure 2. Moreover, the FT-IR spectrum of B-H

Table 1 Typical values of physical properties of the carbon sleeves and their antioxidants.

	A-H	B-H	C-H	D-D	E-W	F-T
Density (g cm^{-3})	1.83	1.83	1.78	1.86	1.73	1.85
Hardness (Shore D)	55	59	55	36	57	65
Electrical resistivity (μΩ m)	9.6	13.4	14.3	5.6	13.6	11.3
Coeff. of thermal expansion ($\times 10^{-6}$ °C^{-1})	4.1	4.6	4.5	2.5	3.9	5.2
Apparent porosity (%)	10.8	9.3	12.9	13.8	15.3	12.5
Antioxidant	Phosphate compound	Phosphate compound	Phosphate compound	Phosphate compound	Phosphate compound	Silicon compound

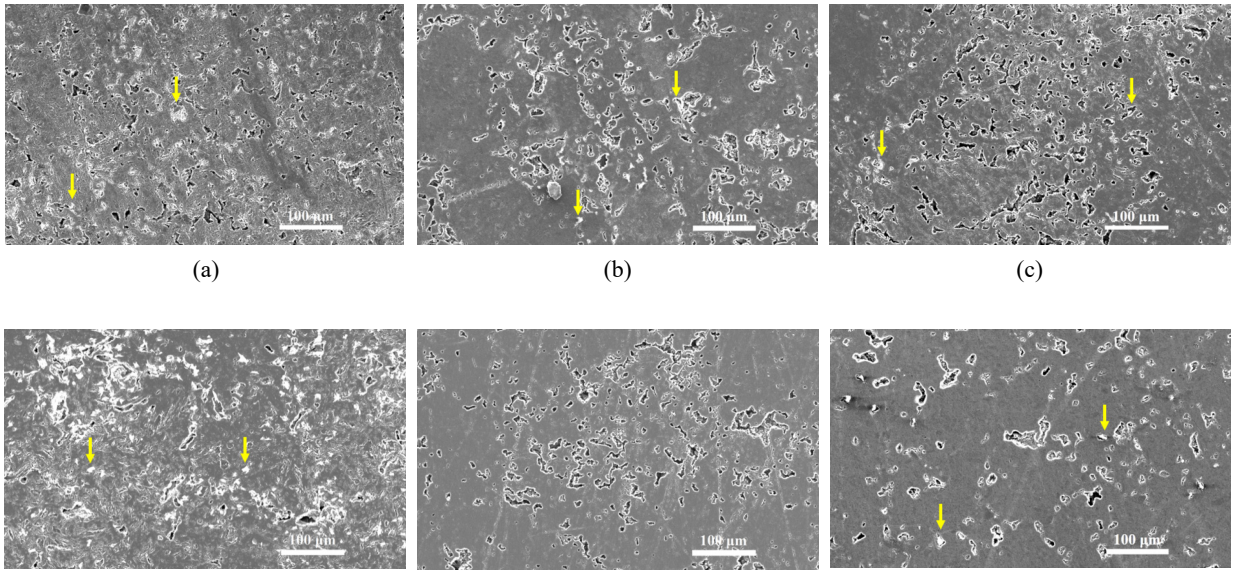

(a) (b) (c)

(d) (e) (f)

Fig.1. SEM micrographs of (a) A-H, (b) B-H, (c) C-H, (d) D-D, (e) E-W, and (f) F-T. Yellow arrows indicate antioxidant deposits.

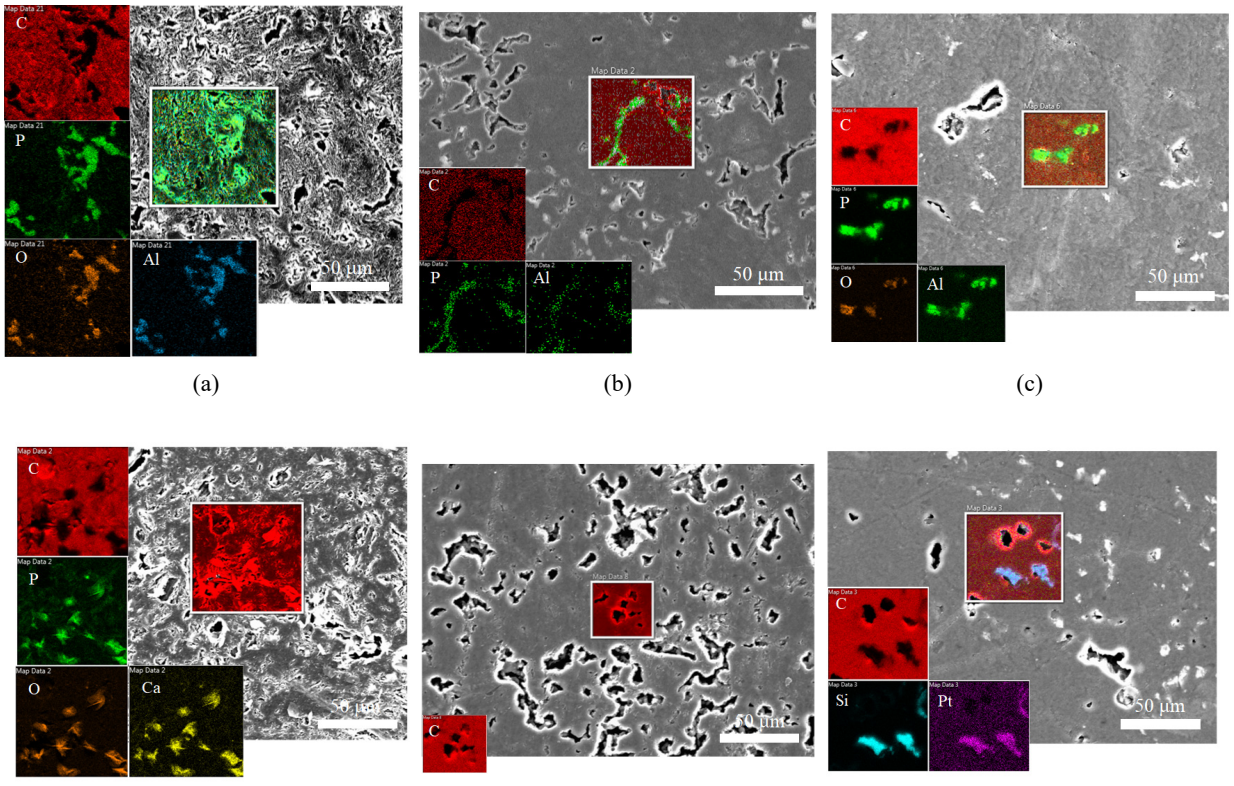

(a) (b) (c)

(d) (e) (f)

Fig.2. SEM micrographs and EDX maps of (a) A-H, (b) B-H, (c) C-H, (d) D-D, (e) E-W, and (f) F-T.

exhibited a broad peak ranging from 3500 to 3300 cm^{-1} from the O-H group, and a small peak at 1580 cm^{-1}, most likely due to the adsorbed water. This indicates that the B-H sample contains more hydroxyl groups and has a higher tendency to adsorb water.

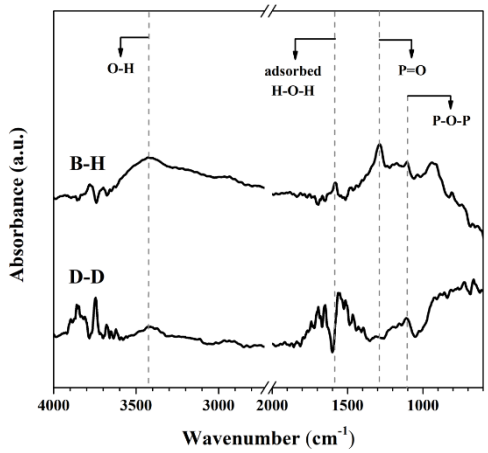

Fig.3. FT-IR spectra of the B-H and D-D samples.

3.2 Oxidation Kinetics Analysis Results

The oxidation rate of the samples at high temperatures, such as at 800°C, was measured using TGA, and the results are displayed in Figure 4. The oxidation rate of E-W, which has no obvious antioxidants deposited, is relatively high. By applying proper antioxidation treatments, the oxidation reaction could be suppressed, as revealed by the lower oxidation rate of the A-H, B-H, C-H, D-D, and F-T samples. According to Figures 1 and 4, it was found that the increase in antioxidation ability was affected by the morphology of the antioxidant deposit. For the A-H, B-H, and C-H samples, the voids tended to be entirely sealed by the antioxidants, and thus their antioxidation ability was greatly enhanced. For D-D, however, the sealing of the voids was not as complete as that within A-H, B-H, and C-H, so that the oxidation rate of the D-D sample was slightly higher. It was deduced that the precipitation of the phosphate compounds in D-D was fast, so that the particle size of antioxidants was large and the precipitates had difficulty filling the voids. For the F-T sample, the deposited antioxidants scarcely filled the voids, and its antioxidation ability was inferior to that of the A-H, B-H, C-H, and D-D samples. This suggests that only a small amount of silicon compounds precipitated within the voids during its antioxidation treatment.

3.3 Field Test Results and Discussion

Some rollers covered with A-H, B-H, and F-T, respectively, have been prepared and deployed in 3ACL for field test. These rollers were installed in the heating zone with a temperature of around 1000°C, and after a period of time (about 6 months), these rollers were detached to examine the extent of oxidation. Figure 5 shows the sleeves after the field test. The sleeve of A-H was obviously corroded, while there were no oxidation marks on B-H and F-T. The sleeves were then

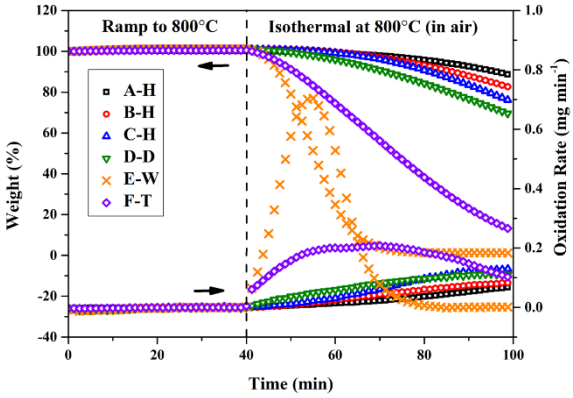

Fig.4. Weight loss profiles and oxidation rate of (a) A-H, (b) B-H, (c) C-H, (d) D-D, (e) E-W, and (f) F-T.

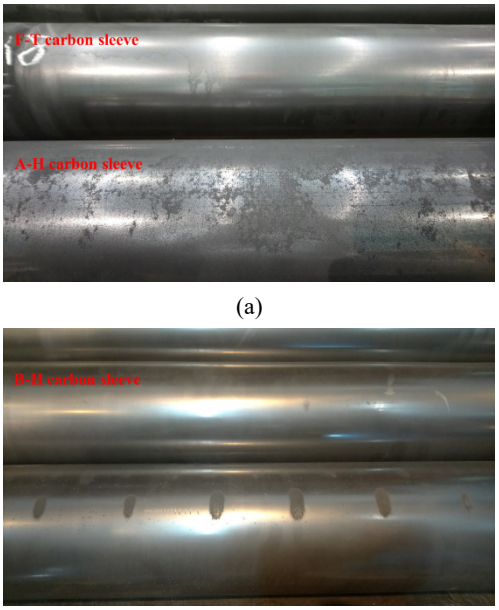

Fig.5. Images of the carbon sleeves of (a) F-T, A-H, and (b) B-H after the field test.

removed to inspect the metal core cylinders, as displayed in Figure 6. The cylinders covered with A-H and B-H were found to be seriously corroded, while those covered with F-T remained intact.

Since phosphate compounds tended to hydrolyze at high temperatures even though the water content in the atmosphere was quite low, it was inferred that the corrosion of the metal core cylinders covered with A-H and B-H was mainly caused by the hydrolysis of phosphate compounds, which could leach out phosphoric acids and thus corrode the roller cores. For the sleeves of A-H and B-H, as the phosphate compounds hydrolyzed and the antioxidants reduced, their antioxidation ability gradually declined, and the sleeves became vulnerable to

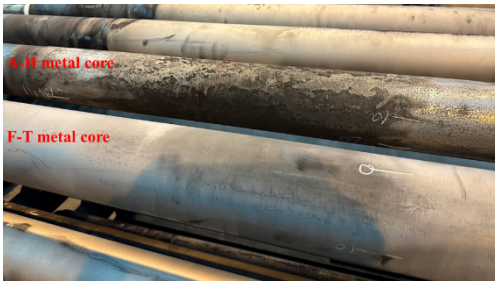

(a)

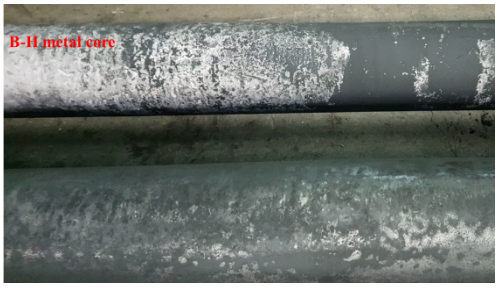

(b)

Fig.6. The images of the metal core cylinders covered with (a) F-T, A-H, and (b) B-H after the field test.

oxidation. It is reasonable to believe that during the field test, the oxygen content in the atmosphere was extremely low, such that the antioxidation treatments for A-H, B-H, and F-T were all sufficient to resist oxidation at such a high temperature. However, it was the reduction of phosphate compounds in A-H and B-H that damaged their antioxidation ability.

In Figure 5, it can be found that the sleeve of B-H exhibited a better antioxidation ability than that of A-H. According to Figure 2 and Table 1, the number of pores in B-H is fewer and their pore size is smaller. This could probably make the phosphate compounds in the B-H sample more difficult to hydrolyze and thus retarded the oxidation of B-H.

To further verify if the corrosion of the metal core cylinders was caused by the leaching out of phosphate compounds, the scale on the metal cores was collected for SEM analysis. Three kinds of scale, which came from scarcely corroded, mildly corroded, and severely corroded metal cores, have been investigated. Their SEM micrographs, along with the EDX spectra, are shown in Figure 7. The scarcely corroded metal was

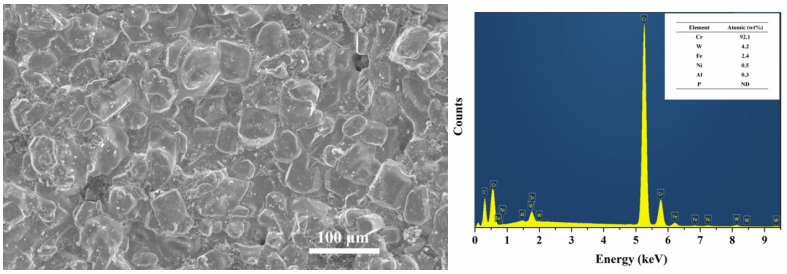

(a)

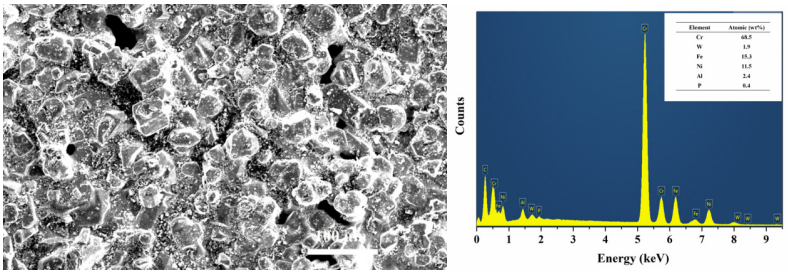

(b)

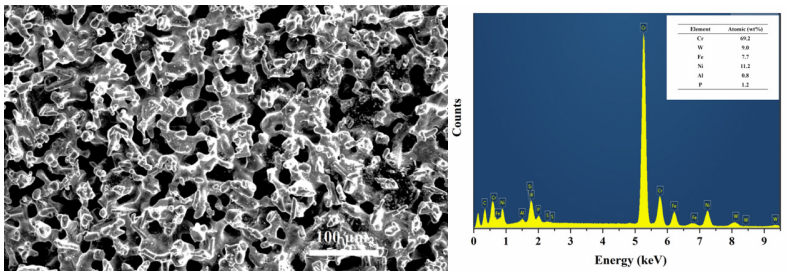

(c)

Fig.7. SEM micrographs and EDX spectra of scale collected from (a) scarcely corroded, (b) mildly corroded, and (c) severely corroded metal core cylinders.

found to be composed mainly of chromium (Cr), tungsten (W), iron (Fe), nickel (Ni), and other trace elements, as displayed in Figure 7 (a), but the phosphorus (P) element was hardly observed. The metal cores exhibited quite intact columnar crystal texture, suggesting that most of the crystalline structure observed in Figure 7 (a) could be attributed to the pristine metal core cylinders. For the mildly corroded metal, the columnar crystals were slightly eroded with some debris left on the scale, and phosphorus (P) element was vaguely observed as shown in Figure 7 (b). For the severely corroded metal, the columnar crystals have almost been completely eroded, and the scale was the residue that demonstrated porous morphology as displayed by Figure 7 (c). On this scale sample, the phosphorus (P) and aluminum (Al) elements were obviously detected, which strongly implied that the corrosion of the metal core cylinders could be induced by the hydrolysis of the phosphate compounds deposited within the carbon sleeves.

4. CONCLUSIONS

Several carbon sleeves made of bulk graphite, followed by the application of different antioxidation technologies, have been fabricated. It was found that the sleeves with their pores entirely sealed by the antioxidants had superior antioxidant ability. The graphite materials impregnated with phosphate compounds were more likely to fill the pores, and their oxidation resistance was significantly improved compared to those without proper treatments. However, the phosphate compounds were found to be prone to hydrolysis at elevated temperatures and leaching out of phosphoric acids. The reduction of phosphate compounds could diminish the antioxidation ability of the sleeves, while the leached-out acids could corrode the metal cores of the rollers. The graphite materials with silicon as the antioxidants, on the other hand, offered a better durability property of a carbon sleeve. Such materials possessed sufficient antioxidation ability, and their silicon deposits did not leach out, which makes the rollers able to retain strong performance properties and extend their service time.

REFERENCES

1. M. Imose: Heating and Cooling Technology in Continuous Annealing, ISIJ, 1985, vol. 25, pp. 911-932.
2. Q. Guo; J. Song; L. Liu et al: Oxidation Protection of Graphite and B4C-Modified Graphite by a SiC Coating, Carbon, 1999, vol. 37, pp. 147-163.
3. W. Lu; D. D. L. Chung: Oxidation Protection of Carbon Materials by Acid Phosphate Impregnation, Carbon, 2002, vol. 40, pp. 1249-1254.
4. T. Đurkić; A. Perić; M. Laušević et al: Boron and Phosphorus Doped Glass Carbon: I. Surface Properties, Carbon, 1997, vol. 35, pp. 1567-1572.
5. D. P. Burduhos-Nergis et al: Characterization of Zinc and Manganese Phosphate Layers Deposited on the Carbon Steel Surface, IOP Conf. Ser.: Mater. Sci. Eng., 2020, vol. 877, 012012.
6. Y. M. Moustafa, K. El-Egili: Infrared Spectra of Sodium Phosphate Glasses, J. Non-Cryst. Solids, 1998, vol. 240, pp. 144-153.